Anal. Chem. **2009,** *81,* 420–426

Improvement of Inner Filter Effect Correction Based on Determination of Effective Geometric Parameters Using a Conventional Fluorimeter

Qun Gu[†] and Jonathan E. Kenny*[,‡]

Department of Chemistry, Edinboro University, Edinboro, Pennsylvania 16412, and Department of Chemistry, Tufts University, 62 Talbot Avenue, Medford, Massachusetts 02155

The most widely used correction of fluorescence intensities for inner filter effects in conventional (90°) fluorimeters fails at high absorbance values. We have critically examined this failure, which is caused by the difference between the geometrical parameters (GPs) of the excitation and emission beams in the typical instrument (focused beams) and in the theoretical picture on which the correction is based (collimated beams). We provide two types of experimental measurement of GPs and show that their substitution in the correction equations leads to significant improvements in the linear range of corrected fluorescence. We also demonstrate that mathematical optimizations give greater improvements and that the optimizations yield GPs consistent with experimental measurements. For solutions exhibiting primary inner filter effect only, we have extended the range of linearity of corrected fluorescence to a_{ex} (absorbance per cm) up to 5.3; for systems with both primary and secondary inner filter effects we have achieved linearity for $a_{ex} + a_{em} = 6.7$. In all cases linear fits have slopes which agree well with the dilute limit. Different series of one- and two-solute solutions were used to demonstrate effectiveness of our correction methods. We also provide a rationale for the unexpected independence of GPs on excitation and emission bandwidths.

The fluorescence intensity from a sample containing a mixture of noninteracting fluorophores is simply the sum of their separate contributions:

$$F = \sum F_j \tag{1}$$

Chemometric methods of untangling the separate fluorescence contributions of the components may be substituted for physical separation in the laboratory, saving time and money, avoiding exposure of workers to hazardous chemicals and generation of hazardous waste, and facilitating in situ analysis of complicated mixtures (e.g., humic materials, environmental samples, petroleum products) in many cases. Under so-called "ideal" or optically dilute conditions, fluorescence intensity of the *j*th fluorophore is a linear function of its concentration, with zero intercept:

$$F_{\text{ideal},j}(\lambda_{ex}, \lambda_{em}) = k'(\lambda_{ex}, \lambda_{em})\Phi_{f,j}(\lambda_{em})I_0(\lambda_{ex})2.3\varepsilon_j(\lambda_{ex})(\Delta x)(c_j) \tag{2}$$

where $F_{\text{ideal},j}(\lambda_{ex}, \lambda_{em})$ is fluorescence intensity observed at emission wavelength λ_{em} when excited at excitation wavelength λ_{ex}, $k'(\lambda_{ex}, \lambda_{em})$ is an instrument constant dependent on geometrical and optical factors and is a function of λ_{ex} and λ_{em}, $\Phi_{f,j}(\lambda_{em})$ is the quantum yield of fluorescence at λ_{em}, $I_0(\lambda_{ex})$ is the intensity of the excitation light incident on the sample, $\varepsilon_j(\lambda_{ex})$ is the molar decadic absorption coefficient of the fluorophore at λ_{ex}, c_j is the molarity of the fluorophore, and Δx is path length of the excitation beam. These ideal conditions are met when attenuation of light at both λ_{ex} and λ_{em} is negligible over the path lengths of interest. Absorption of excitation and/or emission radiation by a sample reduces fluorescence intensity and results in a nonlinear relationship between the observed fluorescence intensity and the concentration of the fluorophore. This is called the "inner filter effect" (IFE). Primary inner filter effect (pIFE) refers to the absorption of excitation radiation, and secondary inner filter effect (sIFE) refers to the absorption of emission radiation. The latter can be avoided completely if an emission wavelength is used where no component of the sample absorbs light, but pIFE normally can only be minimized, because absorption by the fluorophore must occur to provide the excitation.

Commonly, investigators seek to restore the linear relationship between the fluorescence intensity of the fluorophore and its concentration by multiplying the observed fluorescence F_{obs} by appropriate correction factors

$$F_{\text{ideal}}(\lambda_{ex}, \lambda_{em}) = F_{\text{obs}}(\lambda_{ex}, \lambda_{em})\text{CF}_p(\lambda_{ex})\text{CF}_s(\lambda_{em}) \tag{3}$$

so that eq 2 still holds for F_{ideal}. In eq 3, CF_p is the correction factor for pIFE, which depends on the total absorbance of the sample at λ_{ex}, whereas CF_s is the correction factor for sIFE, which depends on the total absorbance of the sample at λ_{em}. Because the correction factors are wavelength-dependent, chemometric methods of mixture analysis based on reference spectra of components will not give reliable results unless the observed spectra are properly corrected.[1] This includes most methods, such as least-squares, rank annihilation, PARAFAC, and other multiway methods. These methods may still fail if the fluorophores in the sample interact.

* To whom correspondence should be addressed. E-mail: jonathan.kenny@tufts.edu. Fax: 1-617-627-3443.

[†] Edinboro University.

[‡] Tufts University.

(1) Siano, S. A. *J. Quant. Spectrosc. Radiat. Transfer* **1992**, *47*, 55–73.

10.1021/ac801676j CCC: $40.75
Published on Web 12/08/2008

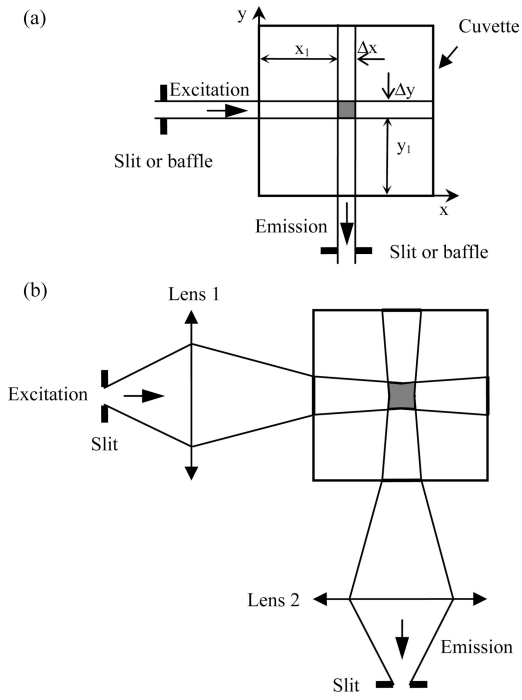

Figure 1. Two cases of OLV in a standard 1 cm cuvette, shown in two dimensions with the *z*-dimension ignored, assuming slit or baffle width of 0.1 cm for both excitation and emission sides. (a) Shape of the OLV, assuming ideal beam condition, geometry of the OLV defined by slit (or baffle) widths. (b) Shape of the OLV, under noncollimated beams condition in a common commercial fluorimeter; the larger OLV and irregular geometry are caused by the refraction of the sample solution.

We focus on the most common case of right-angle geometry; see Figure 1a. Equations for IFE corrections for this geometry have been presented by several groups.[2−4] Recently, MacDonald et al. provided the derivations of IFE correction factors (CF) for both primary and secondary IFE for this geometry.[4] We adopt their symbols because of the completeness and clarity of their work. The simplifying assumptions used in the MacDonald et al. derivations (and apparently most others, although they are not all explicit on this point) include modeling the excitation and emission beams as sharp-edged, uniform, and collimated with rectangular cross sections of known dimensions, $\Delta y \times \Delta z$ and $\Delta x \times \Delta z$, respectively, determined by the slit widths and heights of the excitation and emission monochromators; see Figure 1a. According to MacDonald et al.,[4] the expression for F_{ideal} becomes

$$F_{ideal}(\lambda_{ex}, \lambda_{em}) = k(\lambda_{ex}, \lambda_{em}) I_0(\lambda_{ex}) \Phi_f(\lambda_{em}) 2.3 a_{fex} \Delta x \Delta y \quad (4)$$

where a_{fex} is the absorbance per cm of the fluorophore at λ_{ex}. They derive the following relationship between F_{ideal} and F_{obs}:

$$\frac{F_{ideal}}{F_{obs}} = \frac{2.3 a_{ex} \Delta x 10^{a_{ex} x_1}}{1 - 10^{-a_{ex}\Delta x}} \frac{2.3 a_{em} \Delta y 10^{a_{em} y_1}}{1 - 10^{-a_{em}\Delta y}} = CF_p CF_s \quad (5)$$

where a_{ex} and a_{em} are the values of absorbance of the solution (fluorophore *and* other absorbers, or chromophores according to the language of ref 4) per cm at λ_{ex} and λ_{em}, respectively; x_1 and y_1 are the distances from the edges of the beams to the cell wall, toward light source and toward detector, respectively, as shown in Figure 1a. In this paper, the geometrical parameters or GPs (Δx, x_1, Δy, and y_1) are in units of cm, and we use a to stand for absorbance per cm in order to distinguish it from the conventional A for dimensionless absorbance. In this model, the fluorescence signal arises from molecules in the overlap volume (OLV) of the excitation and emission beams. Besides Δx and Δy, the OLV is also defined by a constant Δz (the slit height) that is included in k in eq 4. The primary correction factor in this equation, CF_p, is consistent with the work of Parker and Barnes[2] and Holland et al.,[3] and the secondary correction factor, CF_s, is analogous. Lakowicz[5] and others have approximated these correction factors as $10^{a_{ex}x_1}$ and $10^{a_{em}y_1}$, respectively, with $x_1 = y_1 \approx 0.5$ cm, for the typical 1 cm square cuvette, giving the convenient expression

$$CF_p CF_s \approx 10^{(a_{ex}+a_{em})/2} \quad (6)$$

The success of inner filter corrections has sometimes been measured by indicating the highest a_{ex}, a_{em}, or $a_{ex} + a_{em}$ value for which the corrected fluorescence remains linear. Little attention has been paid to the value of the slope of the corrected fluorescence, despite its information content (see eq 2).

The corrections represented by eq 5 have been carefully tested by Holland, Christmann, and co-workers.[3,6−8] They built a number of special instruments which simultaneously measured absorbance and fluorescence and were capable of correcting the fluorescence intensities "on the fly." These instruments utilized right-angle geometry with special optical arrangements to produce collimated excitation and emission beams which nearly matched the properties of the ideal beams assumed in the derivation of the correction factors. These instruments were orders of magnitude less sensitive than typical instruments which use tight beam focusing. In the work reported by Christmann et al.,[8] IFE-corrected fluorescence was linear up to $A_{ex} = 2.7$ when only pIFE was involved and linear up to $A_{ex} \approx 2$ and $A_{em} \approx 2$ when both pIFE and sIFE were involved. These maximum absorbances do not necessarily represent any limitations to the theoretical correction factors; rather, the sensitivities of the instruments made measurements of absorbances larger than 2 difficult. In fact, the authors of ref 8 state "No fundamental limitation of the accuracy of the cell shift method is indicated under the conditions of these experiments." This observation does not apply to ordinary instruments without collimated beams.

Most commercial or research instruments use focusing optics to concentrate the excitation beam and to collect a large fraction of the fluorescence emitted from the OLV. Our goal in this work is to investigate and optimize the utility of the most commonly

(2) Parker, C. A.; Barnes, W. J. *Analyst* **1957**, *82*, 606–618.
(3) Holland, J. F.; Teets, R. E.; Kelly, P. M.; Timnick, A. *Anal. Chem.* **1977**, *49*, 706–710.
(4) MacDonald, B. C.; Lvin, S. J.; Patterson, H. *Anal. Chim. Acta* **1997**, *338*, 155–162.
(5) Lakowicz, J. R. *Principles of Fluorescence Spectroscopy*, 3rd ed.; Springer Science and Business Media, LLC: New York, 2006.
(6) Christmann, D. R.; Crouch, S. R.; Holland, J. F.; Timnick, A. *Anal. Chem.* **1980**, *52*, 291–295.
(7) Christmann, D. R.; Crouch, S. R.; Timnick, A. *Anal. Chem.* **1981**, *53*, 276–280.
(8) Christmann, D. R.; Crouch, S. R.; Timnick, A. *Anal. Chem.* **1981**, *53*, 2040–2044.

used correction scheme, eq 5, derived for collimated beams, in conjunction with the most commonly used fluorimeter configuration, utilizing focused beams. Linearization of fluorescence response of optically dense samples, including mixtures of fluorophores, for analytical purposes is one specific objective. Another is to facilitate the study of the photophysics of complicated mixtures, such as petroleum products and humic materials. Interactions among components of such mixtures, such as electronic energy transfer[9] in oils, have been postulated, but without reliable inner filter corrections, identifying the nature of the energy transfer has not been possible.

We critically examine the difference between the GPs of the excitation and emission beams in the typical instrument and in the theoretical picture on which the correction is based. We provide two independent types of experimental measurement of actual GPs and show that their substitution in the correction equations leads to significant improvements in the linear range of corrected fluorescence. We also demonstrate that mathematical optimizations of the GPs can give similar improvements and that the optimizations yield GPs consistent with our experimental measurements. We also investigate the reported independence of effective GPs on the slit widths of the excitation and emission monochromators,[10,11] another experimental observation at odds with the theoretical picture. Our analysis provides a rationale for this observation.

EXPERIMENTAL SECTION

Anthracene (99%, ACROS), naphthalene (99%, ACROS), cyclohexane (HPLC grade, 99.0%, ACROS), ethanol (absolute, ACROS), quinine sulfate dihydrate (99%, ACROS), fluorescein, sodium salt (99%, ACROS), and concentrated sulfuric acid (Fisher, assay 95% to ~98%) were used directly without further purification. The 1 cm and 0.1 cm path length fused-silica cuvettes were obtained from Starna. All fluorescence measurements were conducted on an SLM 4800 fluorimeter (SLM-Aminco). Nominal gain settings of 1, 10, and 100 were found to be correct to within 0.4−1.2% in an experiment monitoring the Raman line of water excited at 350 nm. Linear response of the water Raman line excited at 300 nm was verified to within about 4% using calibrated neutral density filters to attenuate the signal at a given gain setting. Combining the two results ensures linear response to within 5% over at least 4 orders of magnitude of fluorescence intensity. For absorbance measurements, a Cary 300 UV−vis spectrometer was used. Its response from 200 to 700 nm was checked with calibrated neutral density filters. Relative errors in absorbance for the range of 0.3−3.0 absorbance units averaged −3.4% with a standard deviation of 3.8%.

Experimental Design. Several series of solutions were chosen to facilitate a systematic study of IFE. The basic experiment on pIFE over the widest range of sample absorbances was carried out on series A, anthracene in cyclohexane, 18 solutions from 0.1 to 1000 mg/L (5.61×10^{-7} to 5.61×10^{-3} M); measurements at two different excitation wavelengths were performed. In series B, pIFE was studied for the same analyte in a different solvent, ethanol (0.1 to 1000 mg/L). Series C used the same solvent as series A but a different solute: 14 solutions of naphthalene in cyclohexane, 0.1−250 mg/L (7.80×10^{-7} to 1.95×10^{-3} M). Series D extended the pIFE study using a different solvent system, 0.1 N H_2SO_4 in water, and a different fluorophore, quinine sulfate: solutions from 0.2 to 480 mg/L (2.55×10^{-7} to 6.13×10^{-4} M). In series A−D, emission was monitored at a wavelength outside the absorption band of the analyte, to avoid sIFE. Series E was prepared to permit study of solutions with both pIFE and sIFE, based on the correction for pIFE determined in series D. The same solute, solvent, and emission wavelength as in series D were used, and the added chromophore, fluorescein, was the only absorber at the emission wavelength. We show below that it is mathematically convenient to determine GPs for sIFE by using serial dilutions of a stock solution containing both solutes, i.e., ensuring that the dilution factors of both absorbers were the same in each solution studied. So we used 500 mg/L (6.39×10^{-4} M) of quinine sulfate (as fluorophore) and 65 mg/L (1.73×10^{-4} M) of fluorescein (as chromophore) in the stock solution and employed dilution factors of 0, 0.0002, 0.0004, 0.0006, 0.0008, 0.02, 0.04, 0.06, 0.08, 0.12, 0.16, 0.20, 0.24, 0.28, 0.32, 0.36, 0.40, 0.44, and 0.48. Finally, series F focuses on sIFE in a dilute solution of quinine sulfate (3.31 mg/L, or 4.23×10^{-6} M) with a small and constant pIFE and a concentration of fluorescein varying from 0 to 40 mg/L (0 to 9.57×10^{-5} M), namely, 0, 5, 10, 14, 18, 20, 24, 28, 32, 36, and 40 mg/L. Preliminary studies of the absorbance and fluorescence spectra of all the solutes used were performed for the purpose of choosing proper excitation and emission wavelengths, as shown in Supporting Information Figures S-1−S-3. λ_{ex} for each fluorophore was chosen at either a peak or valley in the spectrum to minimize polychromatic effects. λ_{em} for pIFE experiments (series A−C) was chosen at a wavelength where the solution does not absorb. λ_{em} for sIFE study (series E and F) is chosen where the absorption of chromophore is at a maximum.

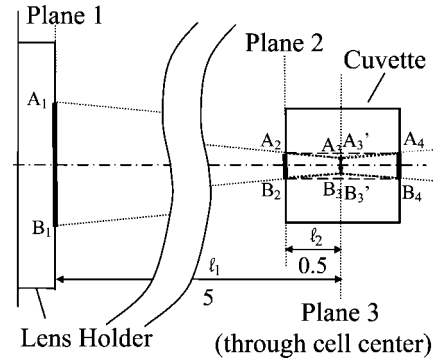

Figure 2. Beam trace in the sample chamber of an SLM 4800 fluorimeter (viewed from the top as in Figure 1); unit: cm. One "edge" of the ray goes through points $A_1-A_2-A_3-A_4$, and the other goes through $B_1-B_2-B_3-B_4$. A_3B_3 is the "beam waist" in air, and $A_3'B_3'$ is the waist when the cell is filled with the solvent cyclohexane.

Ray Tracing and Beam Profiling. The beam width of excitation radiation at 400 nm for the SLM 4800 at the front plane of the lens holder, plane 1 in Figure 2, was measured with a ruler. The beam waist in air at cell center (plane 3) was measured by scanning a micrometer-mounted power meter with pinhole aperture (diameter 50 μm) along the emission optic axis with step

(9) Ralston, C. R.; Wu, X.; Mullins, O. C. *Appl. Spectrosc.* **1996**, *50*, 1563–1568.
(10) Subbarao, N. K.; MacDonald, R. C. *Analyst* **1993**, *118* (7), 913–916.
(11) Kubista, M.; Sjöback, R.; Eriksson, S.; Albinsson, B. *Analyst* **1994**, (119), 417–419.

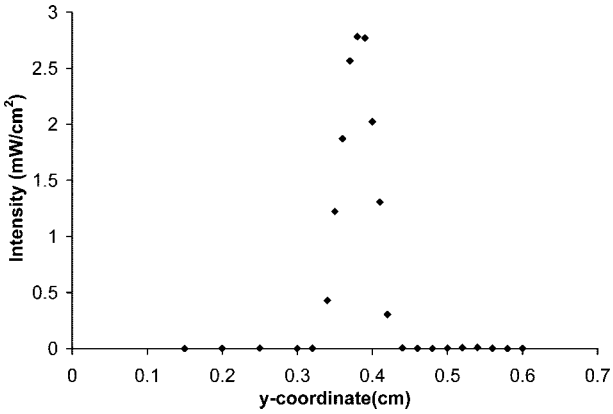

Figure 3. Beam intensity distribution in the *y*-direction in the sample chamber of an SLM 4800 fluorimeter in the approximate focal plane.

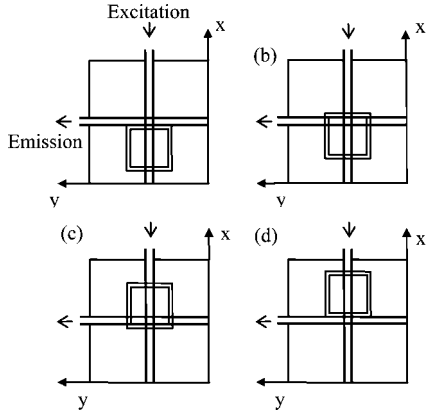

Figure 4. Demonstration of cell shift in the *x*-direction to determine the effective emission beam width Δx. Note the parallel lines represent the effective beams; the beams are not collimated in reality.

size 0.01 cm; see Figure 3. The beam width in plane 3 with the cell filled with solution is calculated using ray tracing with Snell's law, based on the refractive index of the solvent used.

Cell Shift Experiments. A custom-made cell shifting device, a micrometer driven 2-D stage (Newport) mounted with a standard 1 cm cuvette, was adapted to the sample chamber of the fluorimeter for determination of effective GPs Δx and Δy. Cell shifting was performed with λ_{ex} at 313 nm and λ_{em} at 400 nm. The excitation and emission bandwidths were both set at 4 nm. While the *y*-coordinate was fixed so that the excitation beam was at the center of the cuvette, the cuvette was driven toward the excitation monochromator at a step size of 0.01 cm, starting at position a and ending at position d in Figure 4. The distance between the two critical positions b and c, where the observed fluorescence intensity just reaches a maximum and just starts to decline sharply, is a function of the effective beam width Δx. An analogous scan was performed in the *y*-direction to determine Δy.

Fluorescence and Absorbance Measurements. All measurements were performed at room temperature. Bandwidths of 4 nm were chosen for both excitation and emission monochromators. The geometric center of the cell mounted on the 2-D stage was placed at the optical center of the sample chamber by adjusting the micrometers to the desired position. Between two fluorescence measurements, the cell was rinsed six times with the solvent, then dried by nitrogen flow while remaining on the sample holder to minimize the possibility of undesired cell displacement. Absorbance was measured for each solution within a few minutes of the fluorescence measurements, using a 1.00 cm cell for low to medium concentrations and a 0.10 cm cell for medium to high concentrations. Several solutions were measured in both cuvettes to determine the actual path length of the nominally 0.10 cm cell. Validity of Beer's law,[12] i.e., linearity of a versus concentration, was verified for the full concentration range of each solute at each λ_{ex} and λ_{em} used. See Supporting Information Figures S-5−S-11 for details.

Empirical Fits of Effective Beam Widths. The experimental methods of measuring the beam widths described above provide physical evidence for the basis of our approach, and the cell shift method yields GPs that give substantially improved IFE corrections (see below). The general user may obtain similar, if not superior, results without carrying out such measurements by relying on mathematical optimization of beam parameters, fitting actual fluorescence versus concentration data. These methods can also easily model the possibility of a small displacement of the cuvette center from the optical center, which can be important at very high values of a. Our strategy is to estimate the GPs with a nonlinear fitting function, then to optimize them using a linear fit with attention to the slope value. We proceed by optimizing parameters along the *x*-axis using a system with pIFE only.

Nonlinear Function Fit for Approximate Determination of Δx. When there is only pIFE, the observed fluorescence can be expressed as F_{ideal}/CF_p:

$$F_{obs} = k\Phi f I_0 \frac{a_{fex}}{a_{ex}} \Delta y 10^{-a_{ex}x_1}(1 - 10^{-a_{ex}\Delta x})$$

$$= K_p 10^{-a_{ex}x_1}(1 - 10^{-a_{ex}\Delta x}) \quad (7)$$

where a number of factors that are kept constant in the experiments with no sIFE (series A−D) have been collected into a new constant, K_p. Note that x_1 is not an independent variable. For the standard 1 cm cuvettes used in this work, $x_1 = (1 - \Delta x)/2$ if the cuvette is properly centered. If we consider dx, the possible displacement of the cuvette center from the optical center in the *x*-direction, we have $x_1 = (1 - \Delta x)/2 - dx$, giving

$$F_{obs} = (K_p)(10^{-a_{ex}((1-\Delta x)/2-dx)})(1 - 10^{-a_{ex}\Delta x}) \quad (8)$$

With inputs of data pairs of (F_{obs}, a_{ex}) applied to eq 8, the parameters K_p, Δx, and dx can be obtained by a nonlinear function fit routine provided by a program such as R-project.[13] This equation was used with data from solution series A−D for the determination of Δx and dx.

Nonlinear Function Fit for Approximate Determination of Δy. When both pIFE and sIFE are present, the treatment of ref 4 gives $F_{obs} = F_{ideal}/(CF_pCF_s)$. In series E, we correct for pIFE using the effective beam parameters (Δx, dx) found in series D, to get partially corrected fluorescence intensities

(12) Skoog, D. A.; Holler, F. J.; Nieman, T. A. *Principles of Instrumental Analysis*, 5th ed.; Saunders College Publishing: Orlando, FL, 1998.

(13) R Development Core Team. R: A Language and Environment for Statistical Computing; Vienna, Austria; ISBN: 3-900051-07-0; http://www.R-project.org.

$F_{obs}CF_p$. These intensities are set equal to F_{ideal}/CF_s to permit determination of Δy:

$$F_{obs}CF_p = \frac{F_{ideal}}{CF_s}$$

$$= kI_0\Phi_f\Delta x\frac{a_{fex}}{a_{em}}(10^{-a_{em}y_1})(1-10^{-a_{em}\Delta y})$$

$$= (K_s)(10^{-a_{em}y_1})(1-10^{-a_{em}\Delta y}) \quad (9)$$

where we have again collected a number of factors that are constant into K_s. Note that $(a_{fex})/(a_{em})$ is not generally constant in a solution with multiple components, but we prepared the series E solutions as dilutions from a single stock solution containing a fixed ratio of fluorophore to chromophore, so *under these special circumstances, the ratio is constant*. If we consider dy, the possible displacement of cuvette center from the optical center in the *y*-direction, with $y_1 = (1 - \Delta y)/2 -$ dy, we have

$$F_{obs}CF_p = (K_s)(10^{-a_{em}((1-\Delta y)/2-dy)})(1-10^{-a_{em}\Delta y}) \quad (10)$$

This equation was used in the nonlinear fit routine to obtain values for Δy and dy.

Linear Optimization. Approximate GPs (Δx, x_1, *or* Δy, y_1) from the nonlinear fits above were used to determine the search space in the linear optimizations. For series A−D, we implemented a simple Matlab program to step through each possible value of Δx, dx pair, to calculate CF_p using measured a_{ex} according to

$$CF_p = \frac{\ln 10 a_{ex}\Delta x}{10^{-a_{ex}x_1}(1-10^{-a_{ex}\Delta x})} \quad (11)$$

which follows from eq 5. Fluorescence intensity was corrected for pIFE for each concentration of the series, and then a curve of "primary-corrected fluorescence" F_{pCorr} versus a_{ex} was obtained for each pair of trial values of Δx and dx. The linearity and accuracy of each correction curve were evaluated by calculating R^2 and mErr%, which is the percentage error of slope m of the line of corrected fluorescence (LCF), as compared to the slope of the line of dilute solutions (LDS), defined as

$$\text{mErr}\,\% = (m_{LCF} - m_{LDS})/m_{LDS} \times 100\% \quad (12)$$

With reasonable tolerances, such as $R^2 > 0.99$ and mErr% < 0.5%, as constraints in the Matlab program, we could find the GPs leading to the correction curve with the widest range of acceptable linearity. For correction involving sIFE, series E, the best Δx, dx pair determined in the above procedure was applied for calculation of CF_p, then a similar procedure was performed by stepping through each possible Δy, dy pair, calculating CF_s and correcting the fluorescence intensity for both pIFE and sIFE.

Dependence of GPs on Slit Widths. Some investigators[10,11] have reported that significant differences in slit widths do not affect IFE corrections, indicating lack of dependence of geometric parameters on slit widths. We conducted cell shift measurements to address this issue on 1 mg/L anthracene in cyclohexane for a variety of slit width combinations. For each monochromator, both slits were identical; we measured Δx for excitation slit fixed at 0.100 cm and emission slit widths varying: 0.100, 0.050, 0.025 cm. Then Δy was measured with emission slit width fixed at 0.100 cm and excitation slit varying: 0.100, 0.050, and 0.025 cm.

RESULTS AND DISCUSSION

Ray Tracing and Beam Profiling. The beam width of excitation radiation at 400 nm at the front plane of the lens holder, A_1B_1 in Figure 2, was 1.08 cm. The width of the beam (in air) at the center of the sample chamber (Figures 2 and 3), A_3B_3, obtained visually and in the pinhole/detector profiling experiment, was 0.12 cm, very close to the slit width (0.10 cm) of the excitation monochromator. The beam width at the inner wall of the sample cuvette, A_2B_2, is thus about 0.22 cm. A calculation based on Snell's law shows that A_3B_3 increases somewhat (represented as $A_3'B_3'$ in Figure 2) because of refraction of the solvent. For cyclohexane at 400 nm, $A_3'B_3'$ is 0.15 cm. Thus, at these instrument settings, the noncollimated excitation beam width varies between 0.15 and 0.22 cm as it traverses the cuvette. The "average" beam width is significantly greater than the slit width of 0.10 cm. This observation suggests that inner filter corrections derived from the ideal case of collimated beams will have limited success.

Cell Shift Experiments. As shown in Figure 4, observed fluorescence for a dilute solution should be at maximum when the effective beam is completely inside the cuvette, i.e., from position b to c. The distance between these two positions equals the cell length minus the effective beam width. Supporting Information Figure S-4 shows the cell shift experiments in both *x*- and *y*-directions using an anthracene solution of 1 mg/L, with fluorescence observed at 400 nm. The results are $\Delta x = 0.26 \pm 0.01$ cm and $\Delta y = 0.17 \pm 0.02$ cm. As shown in Table 1, the GPs we found using cell shift results for all series (A1, A2, B, C, D) are identical. The dissimilarity between the Δx and Δy values despite identical excitation and emission slit widths is addressed below.

Results of IFE Corrections. Three methods of IFE correction, all based on eq 5 but utilizing different GPs, were performed for fluorescence data of each series. For correction 1, we used the standard assumption[4] that the slit widths of excitation and emission monochromators defined the GPs. According to SLM-Aminco, a bandwidth of 4 nm corresponds to a slit width of 0.10 cm. Therefore, $\Delta x = 0.10$ cm and $\Delta y = 0.10$ cm. For correction 2, GPs determined by cell shift methods are used. For correction 3, the GPs found by mathematical optimization for different solutes, solvents, and excitation wavelengths are very consistent, with Δx ranging from 0.28 to 0.30 cm and dx = 0 except for one series, naphthalene in cyclohexane, where a cuvette displacement of 0.02 cm was found. The average Δx is 0.29 cm, slightly larger than what was determined by cell shift method. For sIFE, we found $\Delta y = 0.17$ and dy = 0 (series E only). The GPs used and the results for series A−E are listed in Table 1.

Correction for pIFE (Series A−D). Uncorrected and corrected fluorescence intensity values at a constant λ_{em} were plotted

Table 1. Geometric Parameters Determined by Cell Shift, Nonlinear and Linear Optimization, and the IFE Correction Results Using Conventional and Effective Beam Width Methods

				IFE correction results				
series	λ_{ex} (nm)	λ_{em} (nm)	method	dx or (dx,dy)	Δx or (Δx,Δy)	R^{2a}	mErr%[b]	$a_{ex,max}$ or $(a_{ex}, a_{em})_{max}$[c,d]
A1, anthracene in cyclohexane	313	400	1		0.1	0.9997	5.68	2.0
			2		0.26	0.9999	1.96	3.9
			3	0	0.29	0.9989	−0.45	5.2
A2, anthracene in cyclohexane	330	400	1		0.1	0.9999	4.74	1.3
			2		0.26	0.9999	2.49	3.7
			3	0	0.29	0.9991	−0.28	4.9
B, anthracene in ethanol	313	400	1		0.1	0.9998	5.17	2.0
			2		0.26	0.9995	2.86	3.9
			3	0	0.28	0.9997	0.044	4.6
C, naphthalene in cyclohexane	281	337	1		0.1	0.9999	0.678	1.3
			2		0.26	0.9999	1.40	3.9
			3	−0.02	0.30	0.9973	−0.58	4.5
D, quinine sulfate in aq H_2SO_4	340	437	1		0.1	0.9994	4.23	2.1
			2		0.26	0.9998	1.51	3.7
			3	0	0.29	0.9991	−0.18	5.3
E, quinine sulfate and fluorescein in aq H_2SO_4	340	437	1		(0.1, 0.1)	0.9986	4.07	(1.7,1.7)
			2		(0.26, 0.17)	0.9990	1.89	(3.1, 3.0)
			3	(0, 0)	(0.29, 0.17)	0.9994	−0.015	(3.4, 3.3)

[a] R^2: R^2 value of the best correction line. [b] mErr%: best percentage error of the slope of the corrected line in comparison to that of a line of dilute solutions. [c] $a_{ex,max}$: maximum a_{ex} in the linear range of the curve of pIFE-corrected fluorescence intensity versus a_{ex}. [d] $(a_{ex}, a_{em})_{max}$: maximum a_{ex} and a_{em} in the linear range of the curve of pIFE- and sIFE-corrected fluorescence intensity versus a_{em}.

against $a_{ex,}$ of each solution in a given series. Results for series A1 (anthracene solutions in cyclohexane) are shown in Figure 5. For comparison, the line for dilute solutions is shown as an extended dashed line (F_dilute). With correction 1, the corrected fluorescence was linear up to about $a_{ex} = 1.96$, with $R^2 = 0.9997$, mErr% ≈ 5%. With correction 2, good linearity was achieved up to $a_{ex} = 3.92$, with $R^2 = 0.9999$, mErr% ≈ 1.3%, a significant improvement as compared to correction 1. Correction 3 for anthracene in cyclohexane is linear up to $a_{ex} = 5.2$, with $R^2 = 0.9989$, and the error of slope is less than 0.5%. Other series show similar results; see Supporting Information Figures S-12−S-15. Average limits of linearity a_{ex} for the three corrections are 1.7, 3.8, and 4.9, respectively. The mathematically optimized GPs permit linear correction of fluorescence in solutions more than 3 orders of magnitude lower in transmittance at the excitation wavelength than the standard correction.

Correction for sIFE (Series E and F). As described above, series E data were used to optimize effective GPs for sIFE correction 3, whereas series F data were simply used to test the effectiveness of GPs previously determined. Therefore, they will be discussed separately.

For series E, as shown in Supporting Information Figure S-16, correction 1 is linear up to $a_{ex} = 1.7$, with $R^2 = 0.997$, and mErr% < 4.1%. Correction 2 increased the linear range ($R^2 = 0.999$) to $a_{ex} = 3.1$, with mErr% < 1.9%. Correction 3 used primary GPs from series D and yielded optimized values for secondary GPs (see above). With these GPs, corrected fluorescence of series E is linear over the entire range studied, $a_{ex} = 3.4$ and $a_{em} = 3.3$, a significant improvement over results obtained with a collimated beam instrument ($a_{ex} = 2.1$, $a_{em} = 2.0$)[7] for a system containing comparable levels of pIFE and sIFE.

In series F, we follow the approach of Christmann et al.,[6] who determined the linear range as those A values for which deviation from linearity was less than 3%. For correction 1, this corresponded to $a_{em} = 2.2$. Corrections 2 and 3 do not differ significantly,

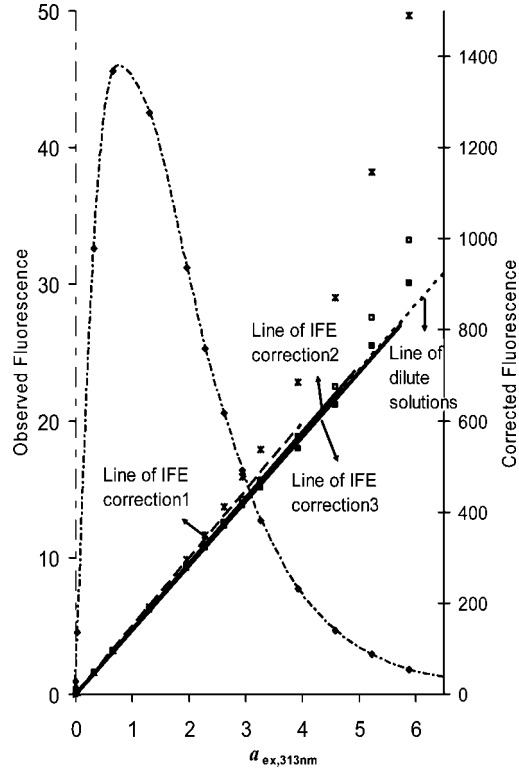

Figure 5. Series A1: λ_{ex} = 313 nm, λ_{em} = 400 nm, anthracene solutions 0.1 to ~1000 mg/L, pIFE only, comparison of corrections 1, 2, and 3. Left scale: uncorrected fluorescence intensity. Right scale: fluorescence intensity of "ideal" (dilute) solutions and of corrected intensity. ∗ correction 1, — line of correction 1, slope = 149.44; □ correction 2, — line of correction 2, slope = 144.13; ■ correction 3, — line of correction 3, slope = 141.30; – – – line of dilute solutions (LDS), slope = 142.28; ♦ observed fluorescence.

because the Δx values used (0.26 cm vs 0.29 cm) do not make much difference when pIFE is low. These corrections remain

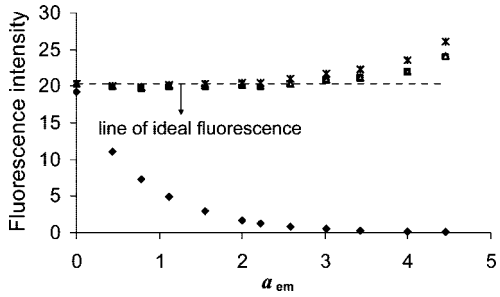

Figure 6. IFE correction for series F: ♦ observed fluorescence, ∗ correction 1, Δ correction 2, □ correction 3, − − − line of ideal fluorescence.

linear with less than 2.9% error up to $a_{em} = 3.0$. The results of the three corrections are shown in Figure 6.

For our corrections to be valid, the systems studied should not display interactions among fluorophores. Evidence for noninteraction among species in these solutions is presented and discussed in the Supporting Information, including absorption spectra at various concentrations in Figures S-17−S-21.

GPs from Cell Shift versus Mathematical Optimization. The mathematical optimization is not expected to yield exactly the same GPs as the cell shift method. The cell shift method measures an effective beam size in one dimension by using a fluorescence measurement; the mathematical optimization simply fits a theoretical expression for a collimated beam to data obtained with a focused beam, all the difference between the two cases being absorbed by the variables.

The values of the effective GPs are related to the optical design and alignment of the instrument and might be expected to depend on the refractive index of the solution. But for the range of wavelengths and solvent refractive indices covered in this study (wavelengths approximately 280−450 nm and refractive index range of 1.32−1.46), it appears feasible to use one series of standard solutions to obtain a common set of effective GPs for IFE correction.

Dependence of GPs on Slit Widths. The results of cell shift measurements using different slit widths dramatically emphasize the difference between the GPs assumed by the theoretical model and those corresponding to conventional fluorimeter which use tight focusing in the sample cell. The cell shift method yields an apparent cross section of the beam that should be a good measure of its size at either cell wall, assuming that the beam is focused at the center of the cell. This beam width, which we have identified as Δy for the excitation beam (Δx for the emission beam), corresponds to A_2B_2 in plane 2 in Figure 2; its value is more dependent on the aperture stop in plane 1 than the value of the slit width for the range of widths studied here. A geometrical optics calculation of this width gives

$$\Delta y = c + bs \tag{13}$$

where b and c are constants and s is the slit width, assuming 1:1 imaging. For our instrument, $c = 0.108$ cm and $b = 0.90$. This gives Δy values of 0.20, 0.15, and 0.13 for the cases in which the experiment yielded 0.17, 0.16, and 0.15 cm, respectively. Similar calculations give Δx values of 0.20, 0.15, and 0.13 cm, corresponding to experimental values of 0.26, 0.27, and 0.27 cm. All experimental values are ±0.02 cm.

The differences between calculated and observed quantities are likely caused by aberrations that affect the properties of the images. Coma and the presence of nonparaxial rays will tend to blur the intensity distribution in the nominal (geometrical optics approximation) image planes of the instrument. On the other hand, finite aperture stops in the beam paths will attenuate the intensity in an image plane, resulting, for example, in the nearly triangular pattern shown in Figure 3 for the excitation beam, rather than the "top-hat" profile expected in the absence of this effect, known as vignetting. The instrument we used in this work has a number of lenses between the excitation monochromator and the final focusing lens, to provide collimated beams for insertion of beam modulation and polarization accessories, so vignetting is likely to be more important in the excitation beam than the emission beam. The difference between Δx and Δy seen throughout this work is consistent with this expected difference in vignetting. To summarize, blurring of the image results in larger image sizes but vignetting reduces the intensity of off-axis image points, so the net effect can be a spot size approximately independent of slit width. Also contributing to the difference may be the wavelength dependence of the focal lengths of the two lenses in the sample compartment: the change in effective focal length of a nominal 5 cm focal length fused-silica lens is 10% over the wavelength range of 230−700 nm.

CONCLUSIONS

The most commonly used correction scheme for inner filter effects, derived for collimated beams, may be used successfully with the most sensitive and most commonly used fluorimeter configuration, utilizing focused beams, if appropriate geometric parameters are used for the effective excitation and emission beam widths. These may be approximated by physical measurements, but the best results are obtained by mathematical optimization, which yields linear corrected fluorescence for a values higher by 2−3 units than previously reported. It is convenient that the mathematical result works so well, since it can be arrived at without any modifications to the instrument, and since the results of a single careful set of measurements yields parameters that apparently can be used over a wide range of experimental conditions.

ACKNOWLEDGMENT

We thank Dr. J. Thomas Brownrigg for carrying out the spectrometer characterizations and for helpful discussions.

SUPPORTING INFORMATION AVAILABLE

Additional information as noted in text. This material is available free of charge via the Internet at http://pubs.acs.org.

Received for review August 9, 2008. Accepted November 14, 2008.

AC801676J